Scientific Justification

1. Motivation

While it is well established that super-massive black holes (SMBHs) lie at the center of most, if not all, massive galaxies (Magorrian et al. 1998), the primary mechanism that turns quiescent black holes into active galactic nuclei (AGN) is still heavily debated. Galaxy mergers have long been proposed as a possible triggering mechanism given their effectiveness in dissipating angular momentum and funneling gas to the center of galaxies (Barnes & Hernquist 1991). This can drive both accretion onto the SMBH and growth of the stellar bulge, which would naturally explain the tight correlation observed between the mass of both components (Gebhardt et al. 2000). However, studies of X-ray selected AGN out to $z \sim 2$ have consistently failed to find a link between AGN activity and the disturbed host morphologies indicative of recent merger activity (Grogin et al. 2005; Schawinski et al. 2011; Kocevski et al. 2012). These results are in direct odds with model predictions which suggest galaxy mergers should become the dominant AGN fueling mode at $z \sim 2$, even among moderate luminosity AGN (Hopkins & Hernquist 2006). A major caveat to these findings is that X-ray surveys are not sensitive to heavily obscured AGN. These obscured AGN represent a key phase in the life cycle of galaxies, as it is during this period that SMBHs are predicted to accrete the bulk of their mass and produce most of their feedback into their host galaxies (Hopkins et al. 2006). Furthermore, hydrodynamical merger simulations predict that this obscured phase should coincide with the most morphologically disturbed phase of a galaxy interaction. It is therefore acutely possible that past studies have systematically missed the AGN-merger connection by not sampling the obscured AGN population well.

2. Proposed Observations

To address this potential bias, we propose for WFC3/IR F160W imaging of 40 heavily obscured, Compton-thick AGN at $z \sim 2$. We will use these observations to search for signs of recent merger activity in their host morphologies. As described below, the majority of these obscured AGN are newly discovered and have been identified by their reflection-dominated X-ray spectra. These AGN are sufficiently rare that they are not well sampled by WFC3 field surveys such as CANDELS. The F160W imaging is vital as it provides high-resolution imaging beyond the 4000Å break at $z \sim 2$, revealing bulges, disks, and even interaction signatures for the first time (see Figure 1). Our proposed observations will *increase by a factor of five* our sample of Compton-thick AGN with rest-frame optical imaging at $z > 1.5$, redshifts where galaxy mergers are predicted to be the primary AGN fueling mechanism.

To search for signatures of merger activity, we will employ a visual classification scheme similar to that used in Kocevski et al. (2012) to examine the morphologies of X-ray selected AGN at $z \sim 2$. We will also make use of two-dimensional surface brightness profile fitting using the GALFIT software (Peng et al. 2002) to determine the best-fit Sersic index for each host, which helps constrains their past merger history. An identical analysis will also be carried out on a mass-matched sample of non-active galaxies to determine if disturbed morphologies are more common among the obscured AGN.

X-ray spectroscopy is the most reliable technique for identifying Compton-thick AGN and our current sample is the largest ever compiled with this method at $z \sim 2$. As such, the observations requested here will enable the first large-scale study of the host morphologies of bona fide Compton-thick AGN at this redshift and will help reveal if the long predicted

AGN-merger connection has been missed in the past due to the effects of obscuration.

3. Sample Selection & Current Results

The most obscured, Compton-thick AGN (hereafter CT-AGN) are hidden by extreme column densities ($N_{\rm H} > 10^{24}$ cm^{-2}) of obscuring gas that can absorb even hard X-ray photons. These AGN can still, however, be revealed in X-ray observations via nuclear emission Compton scattered into our line of sight even when the direct X-ray emission is suppressed. This "reflected" emission has a characteristic spectral shape consisting of a flat X-ray continuum and a high equivalent width Fe Kα fluorescence line (Matt, Brandt & Fabian 1996). Using archival *Chandra* data and X-ray spectral fitting, we have identified 83 CT-AGN in the redshift range $0.5 < z < 2.5$. For this analysis we employed new X-ray spectral models from Brightman & Nandra (2011), which correctly account for emission from Compton scattering and include a self-consistent treatment for Fe Kα emission. These models include all of the signatures of Compton-thick obscuration in a single model, allowing us to find CT-AGN in lower signal-to-noise data than previously possible. Examples of our X-ray spectral fits can be seen in Figure 2. A majority of our sample would not have been identified as heavily obscured by past studies as their X-ray hardness ratios appear soft (due to Thompson scattered emission) and their observed luminosities are often suppressed below the standard luminosity limit ($\sim 10^{42}$ erg/s) for AGN selection. The success of our technique was illustrated in Brightman & Ueda (2012), where a total of 41 CT-AGN were found in the *Chandra* Deep Field South (CDFS), 29 of which were detected as heavily obscured for the first time.

Our sample of CT-AGN is drawn from *Chandra* datasets in three fields: the CDFS 4 Msec observations (Xue et al. 2011) and the wider 800 ksec AEGIS-XD (Laird et al. 2009) and 180 ksec C-COSMOS (Elvis et al. 2009) observations. This combination of deep and wide survey data results in a sample that probes both moderate and high luminosity ($\sim 10^{45}$ erg/s) AGN well. The redshift and luminosity distribution of the sample is shown in Figure 3. The sample includes 32 CT-AGN at $z < 1.5$, all of which are covered by the existing F814W imaging in these fields. However, only 11/51 CT-AGN at $1.5 < z < 2.5$ fall within the existing F160W imaging taken by CANDELS. The remaining 40 AGN at $z \sim 2$ that lack F160W imaging are the targets of our proposed observations.

Using existing F814W imaging, we have found tantalizing evidence for a 2.7σ excess of disturbed morphologies among the CT-AGN at lower redshifts ($z \sim 1$) compared to unobscured AGN with similar X-ray luminosities; this can be seen in Figure 4. Our proposed observations will double our sample of CT-AGN with rest-frame optical imaging at $0.5 < z < 2.5$ and increase by a factor of five (from 11 to 51) our sample at $1.5 < z < 2.5$. At the very least, this increase will raise the significance of our result to the 4σ level. However, mergers are predicted to play a greater role in triggering AGN at $z \sim 2$, therefore *we expect an even greater statistical boost by extending this work to higher redshifts.* Furthermore, our proposed observations will allow us to study a robust sample of high luminosity CT-AGN ($L_{\rm X} > 5 \times 10^{44}$ erg/s) for the first time, by tripling the number that currently have rest-frame optical imaging (from 6 to 20). These sources are exceedingly rare in pencil-beam surveys and such samples cannot be compiled from existing WFC3 imaging from CANDELS.

4. Scientific Goals and Objectives

Our proposed observations and subsequent analysis will address the following issues:

What Triggers AGN Activity? Mergers have been invoked widely as an AGN triggering

mechanism, but imaging of X-ray selected AGN have consistently found a lack of disturbed host morphologies out to at least $z \sim 2$ (Schawinski et al. 2011; Kocevski et al. 2012). However, X-ray surveys become increasingly incomplete as a function of AGN obscuration and therefore do not sample well the Compton-thick population. Our newly identified CT-AGN are a unique sample with which to test the merger-AGN feedback picture. Given their high X-ray luminosities (20 sources have $L_{\rm X} > 5 \times 10^{44}$ erg/s) and their heavy obscuration, these AGN are the best candidates to be found near the "blow-out" phase predicted by AGN feedback models. Furthermore, AGN with these luminosities are typically dominated by their nuclear emission, making it difficult to assess their host morphologies. However, heavy obscuration blocks this light in CT-AGN, providing a rare glimpse at the galaxies that lie beneath. We will use our proposed F160W imaging to examine the rest-frame optical morphologies of these galaxies (both visually and quantitatively) to determine if obscured SMBH growth is preferentially associated with merger activity at $z \sim 2$.

Our preliminary findings that obscured AGN at $z \sim 1$ reside in more disturbed hosts conflicts with the recent results of Schawinski et al. (2012), who report that obscured AGN (selected by their excess mid-infrared emission) at $z \sim 2$ predominately have undisturbed, disk-like morphologies. We will determine if these conflicting results are due to differences in our selection techniques. IR selection can be contaminated by star forming galaxies, while X-ray spectroscopy identifies CT-AGN by directly measuring the line of sight obscuration. It is worth noting that only one of our CT-AGN in CDFS would have been selected as an obscured AGN via the infrared excess method employed by Schawinski et al. (2012). The WFC3 observations proposed here would increase our sample of CT-AGN with rest-frame optical imaging at $z \sim 2$ by a factor of five and allow us to extend our analysis to redshifts where galaxy mergers are expected to become the dominant AGN triggering mechanism (Hopkins & Hernquist 2006). This will permit us to directly test the results of Schawinski et al. (2012) using a independent and spectroscopically confirmed sample of CT-AGN.

Testing the Unification Model: In the local universe, a unification paradigm exists, which invokes a torus-like structure that obscures the central engine for some sight lines, and not for others, producing the two observed AGN types. In this scheme AGN obscuration is largely dependent on the viewing angle of the observer (e.g., Antonucci 1993). The torus paradigm has much observational support in the local universe, but the relevance of the unified scheme at higher redshifts is not so clear (Draper & Ballantyne 2011; Page et al. 2011). For example, observations suggest that AGN obscuration is redshift-dependent (e.g. Hasinger 2008), which is not expected in simple unification models. Alternatively, obscured SMBH growth may be a distinct phase in the evolution of galaxies, specifically one in which the AGN expels gas from the galaxy and terminates its star formation activity via feedback processes (Hopkins et al. 2006). A very simple test of these two scenarios is provided by our proposed observations. In the standard unification picture, all AGN would sample the same parent population of host galaxies, regardless of their level of obscuration. In other words, there should be no correlation between CT-AGN and disturbed host morphologies. On the other hand, in the AGN feedback model there should be a strong dependence between obscuration and host properties such as morphology. Our preliminary results at $z \sim 1$ already hint at a connection between obscuration and morphological state, albeit at a marginal statistical significance. Our proposed observations will enable us to confirm this finding by doubling our overall sample of CT-AGN with rest-frame optical imaging.

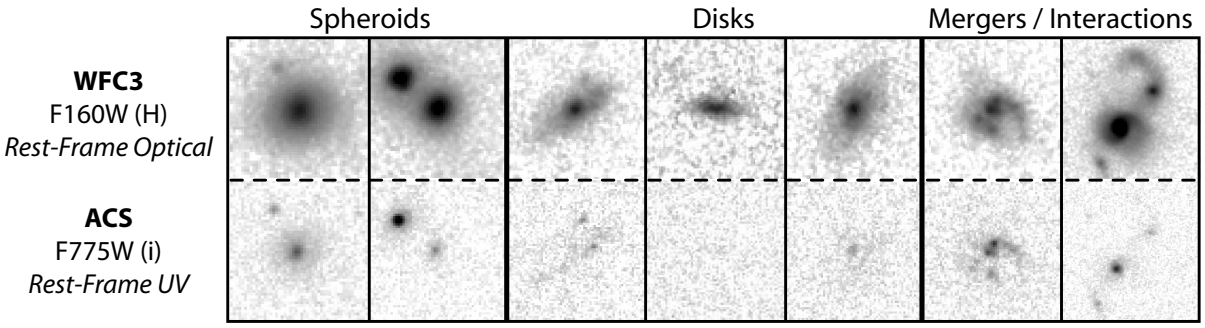

Figure 1: Examples of X-ray selected AGN host galaxies at $z \sim 2$ as imaged by WFC3 in the F160W band (rest-frame optical) are shown above, while ACS observations in the F775W band (rest-frame ultraviolet) are shown below. While ACS observations are sensitive to dust unobscured young stars at this redshift, WFC3 probes light from older stars that dominate the mass budget of galaxies, revealing stellar bulges, disks, and even interaction signatures for the first time. WFC3 imaging is essential if we are to determine the host morphologies of our CT-AGN at $z \sim 2$.

References

Antonucci R. 1993, ARA&A, 31, 473
Barnes, J.E., & Hernquist, L.E. 1991, ApJ, 370
Brightman, M. & Nandra, K. 2011, MNRAS, 413, 1206
Brightman, M.& Ueda, Y. 2012, MNRAS, 423, 702
Draper A.R. & Ballantyne D.R. 2011, ApJ, 740, 57
Elvis, M., et al. 2009, ApjS, 184, 158
Gebhardt, K., et al. 2000, ApJ, 539, L13
Grogin, N.A., et al. 2005, ApJ, 627, L97
Grogin, N.A. et al. 2011, ApJS, 197, 35
Hasinger, G. 2008, A&A, 490, 905
Hopkins, P.F., & Hernquist, L. 2006, ApJS, 166, 1
Hopkins, P.F., et al. 2006, ApJS, 163, 50
Koceski, D.D., et al. 2012, ApJ, 744, 148
Laird, E.S., et al. 2009, ApJS, 180, 102
Magorrian, J., et al. 1998, AJ, 115, 2285
Matt, G., et al. 1996, MNRAS, 280, 823
Page M.J., et al. 2011,MNRAS, 416, 2792
Peng, C.Y., et al. 2002, AJ, 124, 266
Schawinski, K., et al. 2011, ApJ, 727, L31
Schawinski, K., et al. 2012, MNRAS, 425, 61
Xue Y.Q., et al. 2011, ApJS, 195, 10

Description of the Observations

We propose to image 40 newly identified Compton-thick AGN at $z \sim 2$ with WFC3/IR in F160W. These AGN are located in the COSMOS, EGS and CDFS fields, although they fall outside the existing CANDELS F160W imaging in these regions. We request the F160W filter as it samples redward of the Balmer/4000Å break at $z \sim 2$. Unlike ACS observations which are primarily sensitive to dust unobscured young stars at this redshift, WFC3/F160W probes rest-frame optical light from stars that dominate the mass budget of galaxies. This imaging has been shown to reveal stellar bulges, disks, and even interaction signatures in galaxies at $z \sim 2$ for the first time (Grogin et al. 2011). The need for F160W imaging to properly determine the morphologies of galaxies at $z \sim 2$ is demonstrated in Figure 1.

We anticipate that 1-orbit per target is sufficient to assess the morphologies of the CT-AGN host galaxies. This is based on extensive testing done by the CANDELS collaboration using both visual and quantitative morphology measures. Our work with the CANDELS-wide data has shown that with 4/3-orbit of F160W, galaxy morphologies can be reliably determined via visual classification down to H=24.0 mag (AB). Our requested 1-orbit exposures should be sufficient to do the same down to H$\sim$ 23.85 mag (AB). We will use this imaging to both determine the predominant morphological type of each host (disk, spheroid,

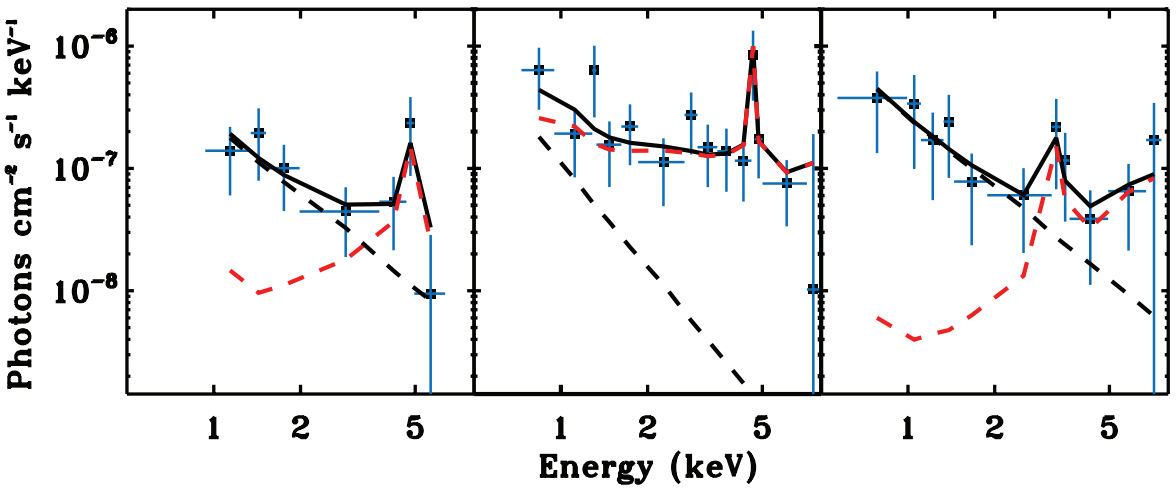

Figure 2: X-ray spectra of three CT-AGN detected in the CDFS 4 Msec observations using the spectral models of Brightman & Nandra (2011). The red dashed line shows the best-fit direct torus emission from the AGN, while the black dashed line shows the Thompson scattered component. Due to heavy obscuration, the scattered component often dominates the emission at low energies, despite typically accounting for $< 1\%$ of the direct emission from these sources. All three sources exhibit strong Fe Kα emission characteristic of CT-AGN.

etc.) and look for signatures of recent merger activity. This includes tidal arms, multiple nuclei, clumpy/patchy structure, and asymmetric/disturbed morphologies. For this analysis we will employ a classification scheme similar to that used in Kocevski et al. (2013). In that study, we showed that interaction signatures could be easily identified in typical AGN hosts at $z \sim 2$ using F160W imaging of similar depth (3000 sec) to those requested here.

Our targets are sufficiently spaced on the sky that we require a unique WFC3/IR observation for each source, necessitating a total of 40 orbits to image the complete sample. The visibility of our targets range from 54 to 57 min. We will split our total exposure into four sub-exposures using the default WFC3/IR 4-point box dither pattern, which is sufficient to fully characterize the PSF. Taking into account WFC3 overheads (guide-star acquisition and exposure overheads), we expect 40/43 min of on-source exposure, split into 4 sub-exposures of 600/645 sec each. Each pointing will be centered on the target CT-AGN and in order to maximize schedulability, we do not place any a priori restrictions on the orientation of the detector for any of the targets.

Special Requirements

Coordinated Observations

Justify Duplications

Past HST Usage

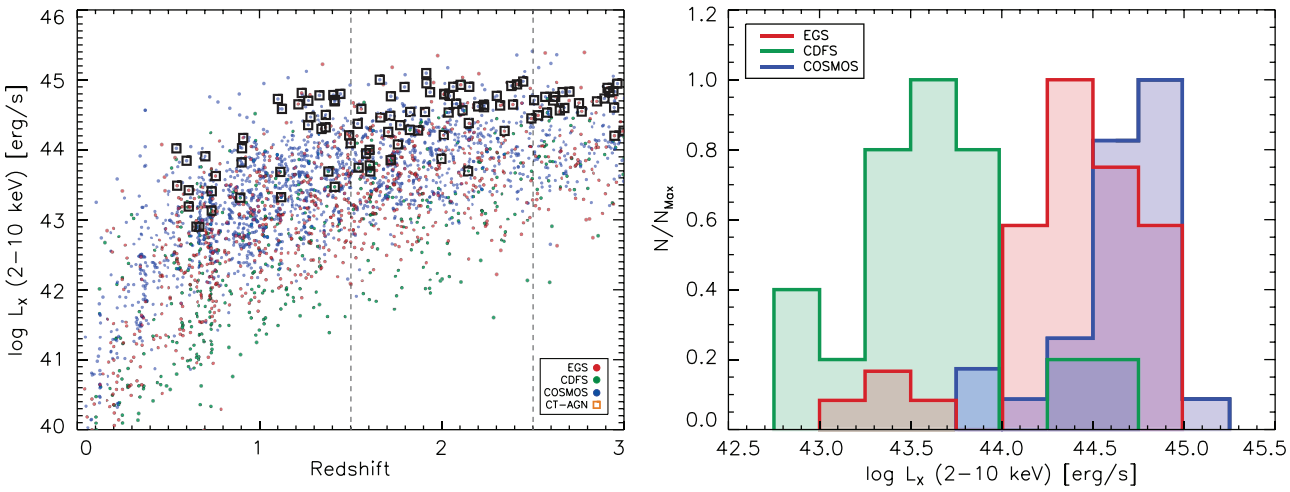

Figure 3: (*left*) Redshift vs X-ray luminosity for X-ray sources detected in the CDFS (red), EGS (green) and COSMOS (blue) fields. Sources identified as CT-AGN by our spectral analysis are noted by the orange boxes. (*right*) Luminosity distribution for the identified CT-AGN in our sample. The use of both deep and wide survey data means our sample includes a large number of high luminosity AGN, which are not well sampled in pencil-beam surveys such as the CDFS 4Ms observations.

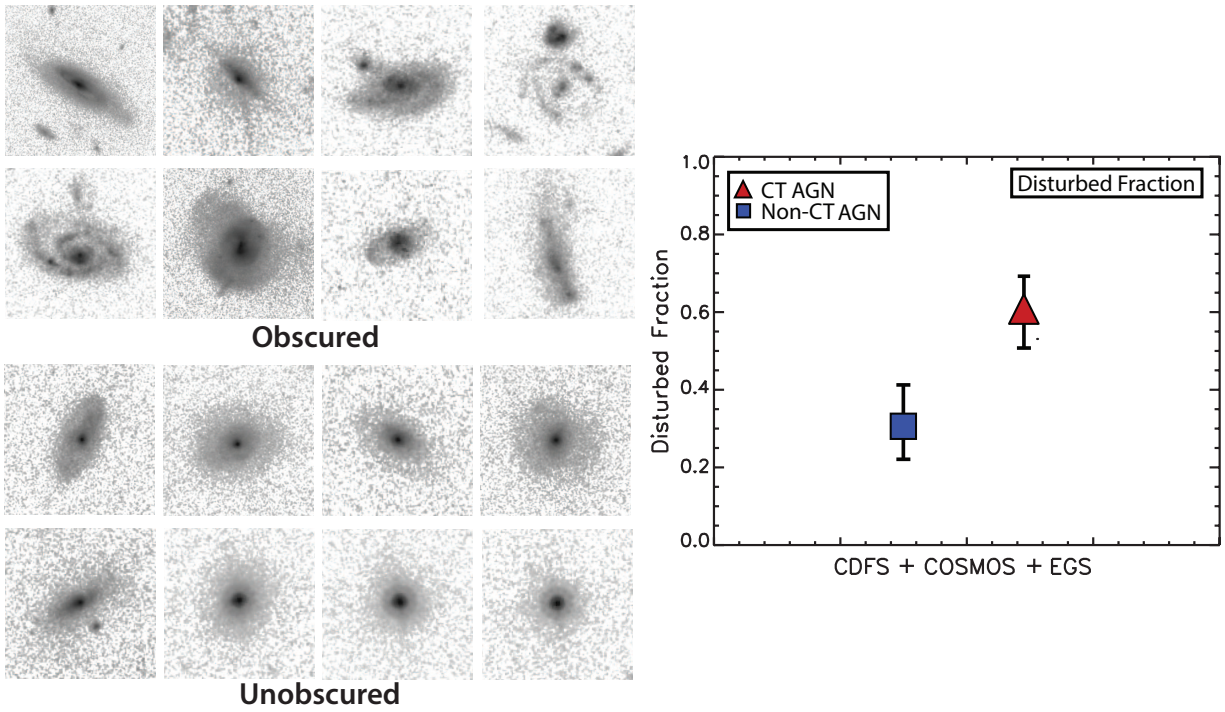

Figure 4: (*left*) ACS/F814W images of galaxies hosting obscured CT-AGN selected by our spectral analysis (top) and a control sample of unobscured AGN (bottom) at $z \sim 1$. Both sets of AGN have similar intrinsic (obscuration-corrected) X-ray luminosities. (*right*) Our preliminary findings suggest heavily obscured AGN reside in more disturbed hosts than their unobscured counterparts at the 2.7σ level. Our proposed observations will double our sample of CT-AGN with rest-frame optical imaging at $0.5 < z < 2.5$ and increase by a factor of five our sample at $1.5 < z < 2.5$, allowing us to extend this work to $z \sim 2$.